Impact of the Alkali Metal on the Structural and Dynamic Properties of the Anionic Pentahydride Ruthenium Complexes [M(THF) x][RuH 5 (PCy 3) 2] (M = Li, Na, K)

Ramaraj Ayyappan, Koushik Saha, Mary Grellier, Eric Clot, Laure Vendier, Sundargopal Ghosh, Sylviane Sabo-Etienne, Sébastien Bontemps

Impact of the alkali metal on the structural and dynamic properties of the anionic pentahydride ruthenium complexes $[M(THF)_x][RuH_5(PCy_3)_2]$ (M = Li, Na, K)

Ramaraj Ayyappan,[a] Koushik Saha,[a,b] Mary Grellier,[a] Eric Clot,[c] Laure Vendier,[a] Sundargopal Ghosh,[b] Sylviane Sabo-Etienne,*[a] Sébastien Bontemps*[a]

[a] LCC-CNRS, Université de Toulouse, CNRS, F-31077 Toulouse Cedex 4, France.

[b] Department of Chemistry, Indian Institute of Technology Madras, Chennai, 600036, India.

[c] ICGM, Univ Montpellier, CNRS, ENSCM, Montpellier, France.

Supporting Information Placeholder

ABSTRACT: A series of anionic ruthenium pentahydride complexes with the general formula $[M(THF)_x][RuH_5(PCy_3)_2]$ (M = Li, Na, K) was synthesized. Their characterization by multinuclear NMR, IR, X-ray diffraction and DFT techniques show that these complexes can adopt different structural features (monomer/dimer, cis/trans phosphines, hydride/dihydrogen ligands) depending on the counter-cation, the solvent and/or the temperature. While the X-Ray diffraction analyses offer snapshots of three out of five isomeric structures found by DFT, the solution and solid-state NMR analysis proved that these complexes exhibit a highly dynamic behavior. Rapid H-D exchange was found between Ru-H and D_2 which was attributed to the presence of Ru-H·····M interactions in the absence of crown-ether.

INTRODUCTION

Transition metal hydrides are key players for a large variety of catalytic reactions and the specific class of polyhydrides offers several opportunities. [1-4,5-8] The presence of dihydrogen ligands or the possibility to establish various types of hydrogen bonding strongly impact activity and selectivity. Neutral and cationic complexes are the most common classes whereas anionic complexes have been much less developed and are more often quite unstable,[9] but they can give a synthetic access heterobimetallic complexes. The field of anionic metal hydride compounds experiences a renewed interest with for example the synthesis of paramagnetic polyhydride iron ruthenium complexes[10-11] or H_2 activation via acceleration of C-H bond reductive elimination by a ruthenium-zinc hydride species.[12]

A convenient way to synthesize anionic polyhydride complexes is by reacting a halogenated metallic precursor with excess alkali hydride reagents such as $LiBHEt_3$, $NaBHEt_3$ or KH in the presence of crown ethers.[13] The role of crown ether is to encapsulate the alkali metal cation, modulate solubility and impart stability. The resulting complexes exist both as separated and contact ion pairs depending on the nature of the solvent and of the crown ether. The anionic and cationic fragments are held together by various interactions including unconventional hydrogen bonding interactions. 21 years ago, Morris *et al.* reported a series of original ruthenium and osmium pentahydride complexes.[14] The ruthenium potassium salts of general formula $[K(Q)][RuH_5(P^iPr_3)_2]$ (Q = 18-crown-6, 1-aza-18-crown-6, 1,10-diaza-18-crown-6) were obtained by reduction of a mixture of $RuCl_3$ and 2.5 equiv. of P^iPr_3 by KH in the presence of various crown ethers under an atmosphere of H_2 (Scheme 1a). Characterization by X-ray diffraction indicated a common feature: the three complexes displayed a pentagonal bipyramidal geometry with the two phosphines in trans position as expected for such bulky ligands (P-Ru-P angles close to 180°) and a pentagon of hydrides. They differed by the establishment of intermolecular proton-hydride bonds between the hydrides and the NH or CH bonds of the various crown-ethers.[14] It should be noted that *in situ* generation of the tricyclohexylphosphine analogue $[K(18\text{-crown-6})][RuH_5(PCy_3)_2]$ was briefly mentioned –without any characterization– ultimately leading to the production of the bis(dihydrogen) complex $[RuH_2(H_2)_2(PCy_3)_2]$ (**1**).[15-16] The formation of another polyhydride anionic Ru complex $\{[(S)Na][Cp^*(^iPr_2MeP)RuH_2]\}_2$ was reported by Tilley *et al.*. In the absence of crown ether, a more complex set of interactions are observed between the anionic Ru and the alkali metal with an eight-membered $[H–Ru–H–Na]_2$ ring (Scheme 1b).[17]

The nature of the counter-cation can have a strong impact in coordination chemistry and catalysis and the alkali metals cannot be always considered as spectator, although their role is somehow difficult to assess.[18-21] Herein, we report the synthesis and characterization of a series of pentahydride complexes [M(THF)x][$RuH_5(PCy_3)_2$] (M = Li, Na, K; x = 1,2)

(Scheme 1c). In the absence of crown-ethers, structural arrangements are shown to highly depend on the nature of the alkali metal and solvent. Based on NMR in solution (THF/toluene) and solid state, X-ray analyses together with DFT calculations, we discuss the highly dynamic behavior observed (monomer/dimer, cis/trans phosphines, hydride/dihydrogen ligands) and the establishment of Ru-H---M bonds.

Scheme 1: a) and b) Relevant reported interactions between anionic ruthenium hydride fragments and alkali moieties. c) General representation of the present work.

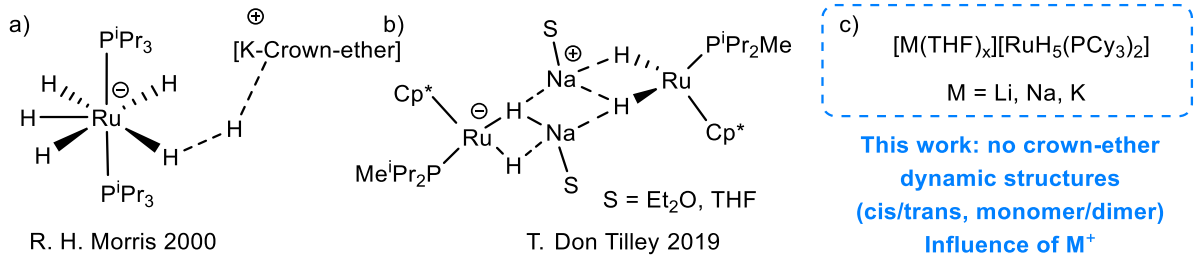

RESULTS AND DISCUSSION

Synthesis and characterization by X-ray diffraction

By reacting the bis(dihydrogen) complex [RuH$_2$(H$_2$)$_2$(PCy$_3$)$_2$] (**1**) with 1 equiv. of LiBHEt$_3$ (1M in THF) at 25°C for 48h, the new complex [Li(THF)][RuH$_5$(PCy$_3$)$_2$] (**2Li**) was isolated after work-up as a white solid in 82% yield.[22] Although, the reaction formally releases H$_2$, we found that conducting it under a pressure of H$_2$ avoids the decomposition observed under Ar. This indicates that the instability of **2Li** is guided by H$_2$ loss.

Scheme 2: Synthesis of complexes 2Li, 2Na and 2K

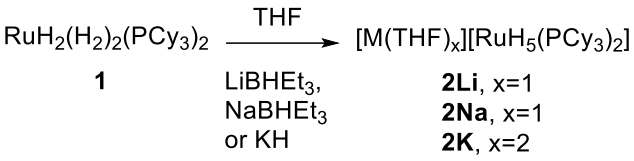

Monocrystals, analyzed by X-ray diffraction, were obtained by layering a concentrated THF solution with n-pentane under H$_2$. The main data are gathered in Table 1. As shown in Figure 1, there are two [RuH$_5$(PCy$_3$)$_2$] anions associated with two Li(THF) units by hydride bridges. Five hydrogen atoms bound to ruthenium were located on the Fourier map in one molecule of the asymmetric unit, whereas only four could be located on the other one. We will only discuss the first metallic fragment. Remarkably for such bulky phosphines, they are found in cis position with a P-Ru-P angle of 114.39(3)°. The ruthenium and lithium atoms are at distances just above the sum of the covalent radii.[23] A THF molecule completes the coordination sphere of each lithium. The structure of **2Li** significantly differs from that of the potassium complexes [K(Q)][RuH$_5$(P^{i}Pr$_3$)$_2$] reported by Morris, in which case, a pentagonal arrangement of the five hydrides was obtained with the two phosphines in trans position (Scheme 1a).[14]

Based on the distances, one can consider that each ruthenium center has one hydride bridging with one lithium (Li2-H201 2.03(5) Å) and another hydride bridging with the two lithium centers (Li2-H204 1.92(3) and 2.02(4) Å), the 8 atoms making a chair arrangement. The triply bridged hydride is roughly trans to a phosphine (H204-Ru2-P4 170 (1)°) whereas the other hydrides are in the equatorial plane together with the second phosphorus atom. Li-H distance of 1.84(5) Å was for example reported in the case of [Li(THF)(Et$_2$O)][Ru(H)-(PCy$_3$)('S4')] ('S4'= 1,2-bis((2-mercaptophenyl)thio)ethane(2-)).[24]

In view of the unexpected geometry of **2Li** in particular with respect to the cis position of the phosphine ligands and Ru-H·····Li interactions, we decided to synthesize the analogous salts [Na(THF)][RuH$_5$(PCy$_3$)$_2$] (**2Na**) and [K(THF)$_2$][RuH$_5$(PCy$_3$)$_2$] (**2K**) by using NaBHEt$_3$ (1M toluene solution) or KH, respectively (Scheme 2). They could be isolated as white solids in 79 and 65 % yield, respectively, and characterized by X-ray diffraction, multinuclear NMR and IR studies. As **2Li**, they are extremely air and moisture sensitive.

Table 1. Selected bond lengths (Å) for 2Li, 2Na and 2K and comparison to DFT values given in *parenthesis*.

	2Li *(2Li-a)*	**2Na** *(2Na-e)*	**2K** *(2K-b)*
Ru2-M^i	2.771(6) *(2.702)*	3.038(1) *(2.983)*	-
Ru2-M	2.806(5) *(2.719)*	3.094(1) *(2.989)*	3.650(2) *(3.598)*
H203-H201	1.59(5) (1.68)	1.00(7) *(0.988)*	-
M-H200	2.39(4) (2.011)	2.34(3) *(2.300)*	2.57(9) *(2.530)*
M-H201	2.03(5) *(2.071)*	2.39(5) *(2.379)*	2.50(8) *(2.530)*
M-H202 M^i-H202	2.26(5) *(2.156)* 2.703(5) *(2.161)*	2.27(4) *(2.161)* 2.28(3) *(2.248)*	-
M-H204 M^i-H204	1.92(3) *(1.933)* 2.02(4) *(2.20)*	2.39(3) *(2.464)* 2.54(3) *(2.593)*	-

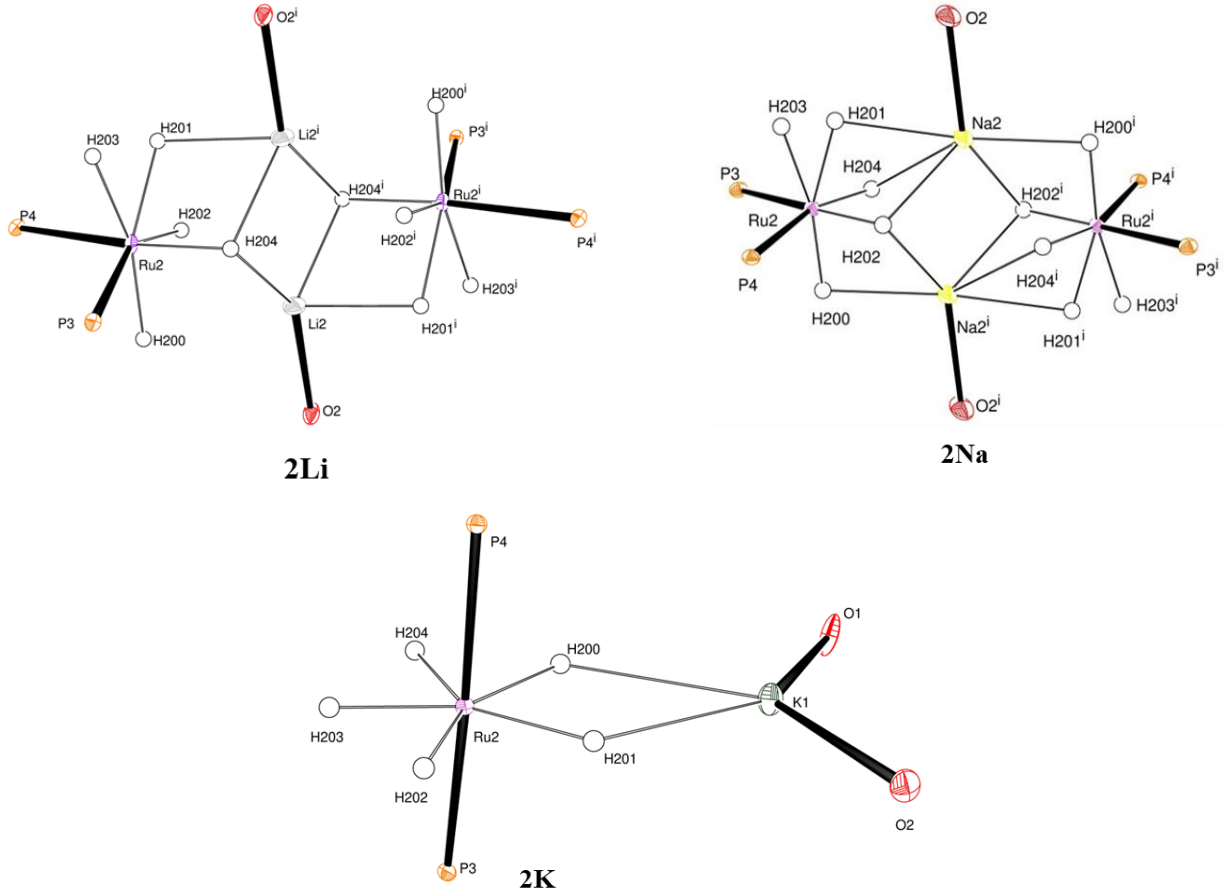

Figure 1. ORTEP views of the X-ray crystal structure of **2Li, 2Na and 2K**. All carbon and hydrogen atoms were removed for clarity, except the hydrides.

If the overall geometry of **2Na** (Figure 1), is similar to that of **2Li**, with a P-Ru-P angle of 114.11(3)°, the hydrides were located in different positions. Facial coordination of hydride ligands with Na2 was present. Each ruthenium atom has one hydride bridging the two Na atoms (Na-H202 2.27(4) and 2.28(4) Å) whereas three other hydrides display slightly longer Na-H distances (2.34(3) to 2.39(5) Å). Similar Na–H distances were reported for the complex described by Tilley *et al.* (Scheme 1b). The authors indicated that each Na atom was in

close contact with three hydride ligands and gave a representation with two full lines (Na-H distances of 2.211 and 2.300 Å) and one dashed line for the longer distance (2.415 Å).[17] A related complex (Na[Ru(H)(py^{bu}S$_4$)]) was reported by Prakash *et al.* to exhibit Na-H distances of 2.160 and 2.215 Å.[25] Importantly, in **2Na**, the two hydrides H201 and H203 are in close contact with a distance of 1.00(7) Å indicative of a dihydrogen ligand bound to ruthenium. The existence of such an isomer was evidenced by DFT calculations (*vide infra*).

2K exhibits a different situation. As shown in Figure 1, a mononuclear structure is obtained with the two phosphines in trans position (P1-Ru-P2 177.63(8)°) and a pentagonal arrangement of the hydrides. The K-Ru distance of 3.650(2) Å is even longer that the one reported for [K(18-crown-6)][RuH$_3$(PPh$_3$)$_3$].THF (3.613 Å) and outside the range of a covalent bond.[26] The potassium is interacting with two hydrides with K-H distances of 2.50(8) and 2.57(9) Å, and its coordination sphere is solvated by two THF molecules. As for **2Li** and **2Na** and in contrast to the related Ru complex reported by Morris *et al.* (Scheme 1a), no crown-ether was used to isolate and stabilize **2K**. We assume that the stabilization is brought by K---H interactions. As a comparison, two crystal structures of trihydride complexes, namely K[RuH$_3$(dcypb)-(CO)][27] and K[RuH$_3$(P(CH$_2$CH$_2$P^{t}Bu$_2$)$_3$)][28] displayed a potassium counterion interacting with all three hydrides with averaged distances of 2.65(5) Å for the first structure and to two hydrides, with distances of 2.55(4) and 2.61(3) Å for the latter structure. These last data can be compared to the reported [K(18-crown-6)][RuH$_3$(PPh$_3$)$_3$][26] exhibiting longer K-H distances (2.57(8), 2.66(8) and 3.13(9) Å) in the presence of a crown-ether isolating the potassium counter-cation. Our recorded solid-state IR spectra of **2M** clearly showed a broad band close to 1730 cm^{-1} corresponding to the Ru-H vibrations. These values are shifted to lower wave-numbers by comparison to the Morris complexes, indicating stronger interactions with the corresponding cations in **2M**, which is expected in absence of crown-ether. The three complexes were too sensitive to obtain reliable microanalytical data.

NMR studies

The three complexes **2Li**, **2Na** and **2K** were characterized in solution by multinuclear NMR analysis in two different solvents, THF-d_8 and toluene-d_8, at variable temperatures as well as in the solid state. The NMR behavior of **2M** proved to be highly fluxional, in contrast to the snapshot situation of the X-Ray diffraction analysis.

In THF-d_8, the three complexes display similar ^{1}H and ^{31}P NMR signals at room temperature: a triplet in the hydride region near –9.5 ppm ($J_{P\text{-}H}$ = 14 Hz; the triplet for **2Na** was only visible at 253K) and a signal above 81 ppm, respectively. In the case of **2Li** and **2K**, upon selective decoupling of the protons of the cyclohexyl ligands, the ^{31}P signal splits into a sextet confirming the presence of 5 hydrides around the ruthenium center. By conducting DOSY experiments, we showed that

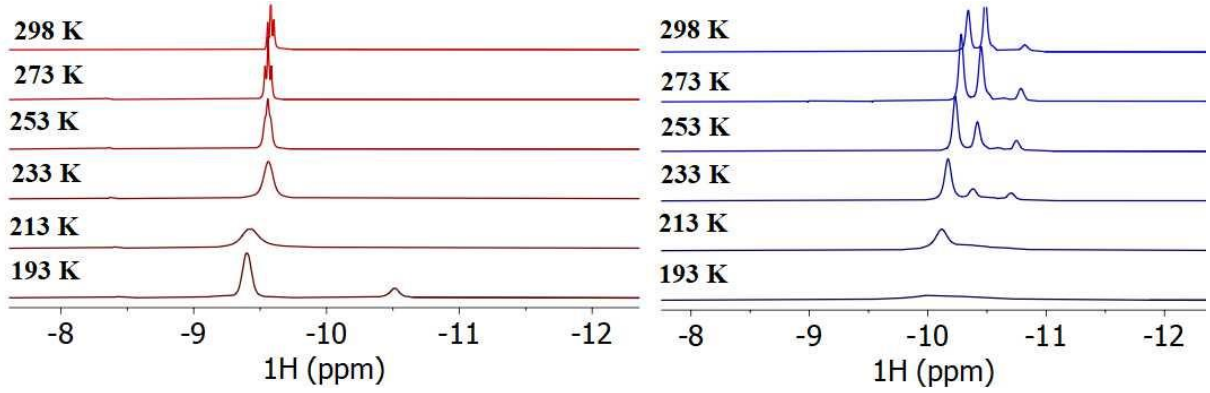

Figure 2. Variable temperature ^{1}H NMR spectral stack plot of **2Li** in, THF-d_8 (Left) or toluene-d_8 (Right).

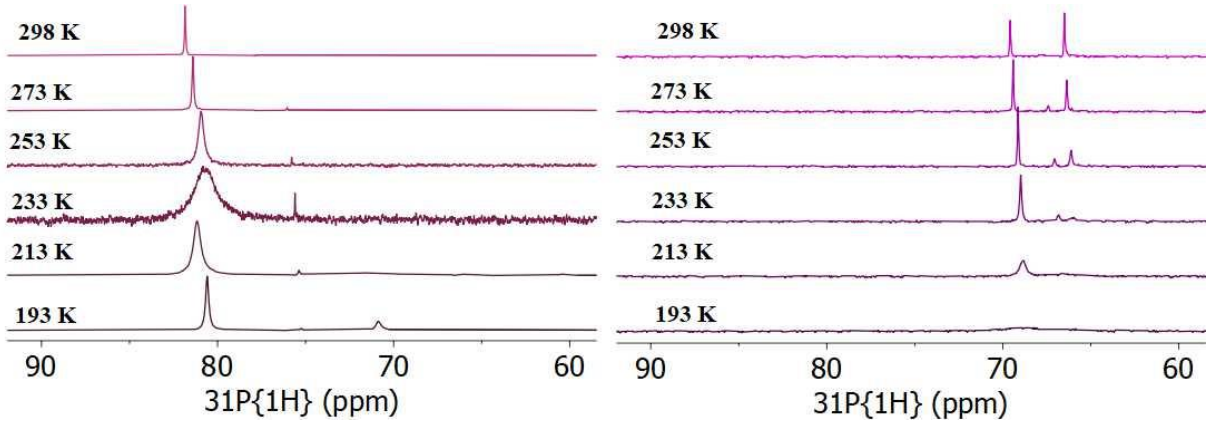

Figure 3. Variable temperature $^{31}P\{^{1}H\}$ NMR spectral stack plot of **2Li** in THF-d_8 (Left) or in toluene-d_8 (Right).

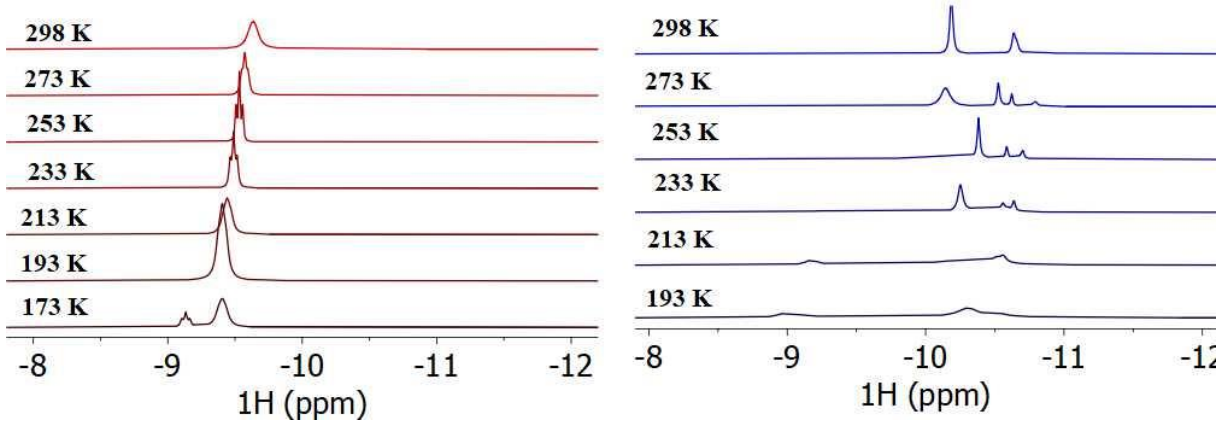

Figure 4. Variable temperature ^{1}H NMR spectral stack plot of **2Na** in THF-d_8 (Left) or in toluene-d_8 (Right).

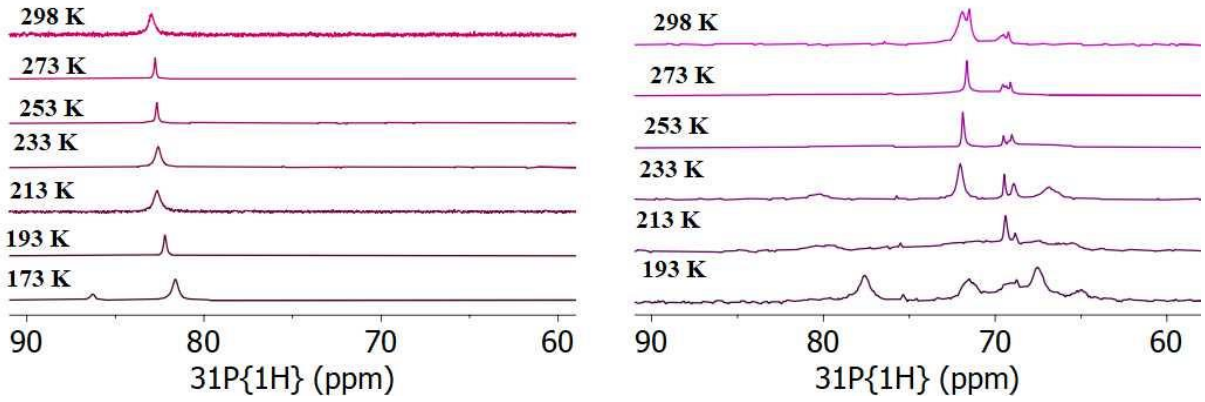

Figure 5. Variable temperature $^{31}P\{^{1}H\}$ NMR spectral stack plot of **2Na** in THF-d_8 (Left) or in toluene-d_8 (Right).

in solution, the dimeric structure characterized by X-ray diffraction for **2Li** and **2Na** dissociates as indicated by diffusion coefficients comparable to the mononuclear ruthenium complexes **1** and **2K.**

Variable temperature NMR monitoring showed significant differences between the complexes. While no change was observed for **2K** by ^{1}H and ^{31}P NMR, (Fig. S31 and S33 in ESI) new signals appeared in the case of **2Li** and **2Na**. For **2Li** (Figure 2, left), the ^{1}H triplet observed at room temperature, broadened and gave two broad signals at –9.40 and –10.51 ppm at temperatures lower than 193K. The Eyring analysis in the temperature range of 183-213K (Figure S7) gave a free energy of activation of 38 kJ.mol^{-1} at 213 K, in acceptable agreement with the barrier of 40 kJ.mol^{-1}, derived from the coalescence temperature. Similarly, at very low temperatures, the ^{31}P NMR analysis gave two signals at 81 and 71 ppm (Figure 3, left). The $^{7}Li\{^{1}H\}$ NMR spectrum gave two broad signals centered at +2.2 and –0.5 ppm together with a sharp singlet at 0.5 ppm. Additional signals appeared at very low temperatures. In contrast, in the case of **2Na**, the ^{1}H broad signal, observed at 298K, sharpened as a triplet, shifted to lower field at 253 K (J(H,P) = 18.2 Hz) and a new broad triplet appeared at –9.13 ppm (t, J(H,P) = 18.2 Hz) (Figure 4, Left), whereas two $^{31}P\{^{1}H\}$ NMR signals at 81 and 86 ppm were detected at 173K (Figure 5, Left).

We conducted T_1 measurements to determine if any dihydrogen ligand could be present in the coordination sphere of the metal center. **2K** provided the highest T_{1min} value of 455 ms at 600 MHz (223K) consisting with a pentahydride formulation whereas lower values were obtained for **2Li** (206 ms at 263K) and **2Na** (220 ms at 253K), all the hydrogen atoms remaining in fast exchange. As we will see hereafter, even lower values were measured in toluene-d_8.

In toluene-d_8, and even at room temperature, the situation is more complex for **2Li** and **2Na** by comparison to the measurements performed in THF-d_8. Several hydride signals (Figures 2, right and 4, right, respectively) appeared in the ^{1}H NMR spectra at room temperature correlating with several $^{31}P\{^{1}H\}$ NMR signals (Figures 3, right and 5, right, respectively) as shown by ^{1}H-$^{31}P\{^{1}H\}$ HMQC NMR experiments (Figure 6 and ESI). Variable concentrations and aging of the solution seem to be important factors to modify the hydride signals ratio in toluene-d_8. Remarkably, for **2Li**, the most intense hydride signals display T_{1min} values around 90 ms at 298K at 600 MHz. Such a low value is in favor of a polyhydride formulation including at least one dihydrogen ligand, but more in-depth studies are needed to conclude on the observed trends, given that longitudinal relaxation times are strongly dependent on the dynamics and on the surrounding environment (ligands, cations, solvent). For **2Na**, the lowest T_{1min} values vary from 126 to 144 ms at 600 MHz for the signals around –10.5 ppm, here also favoring the existence of a dihydrogen ligand, keeping in mind the high fluxionality at all temperatures between several isomers.[29] In contrast, for **2K** in toluene-d_8 solution, the ^{1}H and ^{31}P signals were only shifted. The broad hydride signal resonated at –9.84 ppm and the ^{31}P signal was high-field shifted by 10 ppm (76.2 ppm). Moreover, fast H/D exchange between the hydrides and toluene-d_8 occurred, with half of the hydride signal disappearing after 10 min.

In view of the different structures evidenced by X-ray diffraction, and to the different behaviors shown in solution by NMR experiments, we decided to conduct solid state NMR investigations for the three complexes (see ESI for spectra). The ^{1}H MAS NMR hydride signal for **2Li** appeared rather complex between –8.5 and –10.5 ppm whereas a ^{31}P MAS signal at 75 ppm with a shoulder at 73 ppm and two ^{7}Li MAS signals (1.1 and –0.7 ppm) were observed. In the case of **2Na**, the ^{1}H MAS hydride signal resonates at –10.9 ppm and the ^{31}P MAS signal at 72 ppm with a left-side shoulder. A very broad ^{23}Na MAS signal is centered at –2 ppm. For **2K**, the ^{1}H MAS NMR hydride and ^{31}P NMR MAS signals are observed at –9.3 and 80.8 ppm, respectively. These latter values are intermediate with those obtained in THF-d_8 and toluene-d_8 solutions. Thus, significant differences appear by comparison to solution NMR data, even for those obtained at low temperatures.

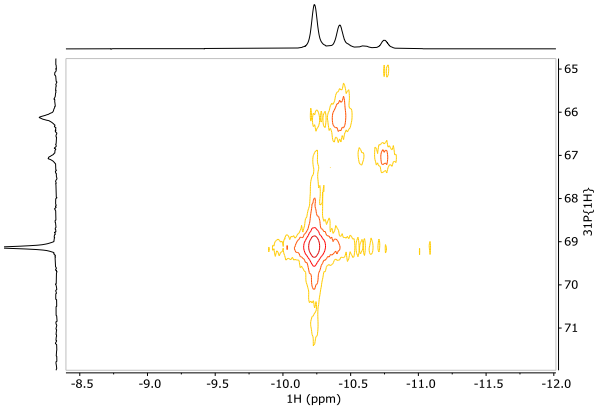

Figure 6. ^{1}H-$^{31}P\{^{1}H\}$ HMQC NMR spectra of **2Li** in toluene-d_8 at 253 K.

Finally, solutions of the three complexes in THF-d_8 were exposed to D_2 gas (1 to 3 bar) at room temperature. Fast H/D exchange was detected by multinuclear NMR experiments conducted on the resulting solutions. Release of H_2 and HD was clearly identified by NMR analysis by their respective signals (singlet at 4.54 ppm and a 1:1:1 triplet at 4.50 ppm with J_{HD} = 43 Hz). For the three complexes **2M**, *ca.* 30% of the initial hydride signal disappeared after 10 min, and up to 90% after 16h. ^{2}H NMR spectra confirmed deuteration incorporation with signals slightly low field shifted. The signals were broad and we could not measure any J_{HD} coupling constants. We noted partial decomposition of **2M** into **1**.

DFT calculations

We conducted full DFT optimization of the three complexes **2Li**, **2Na** and **2K**, employing B3PW91-D3 functional (Figure 7, see ESI for details) with two objectives in mind: i) to compare the hydrogen locations with those obtained by X-Ray diffraction and ii) to explore the structural dynamic behavior of the species depending on the nature of the countercation.

The structures of **2Li**, **2Na** and **2K** were optimized with a good agreement with the X-Ray data and noted **2Li-a**, **2Na-e** and **2K-b**, respectively. The main calculated geometrical parameters are provided in Table 1. The crystal structure of **2Li** is similar to the computed structure of the dimer **2Li-a** with phosphines in a cis position (113.77°). The hydrides adopt the same arrangement and the Li·····H distances range between 1.993 to 2.199 Å following the trend observed by X-ray. The simulation of **2Na** provided the dinuclear structure **2Na-e** featuring also cis phosphines (113.98°). Importantly, as suspected

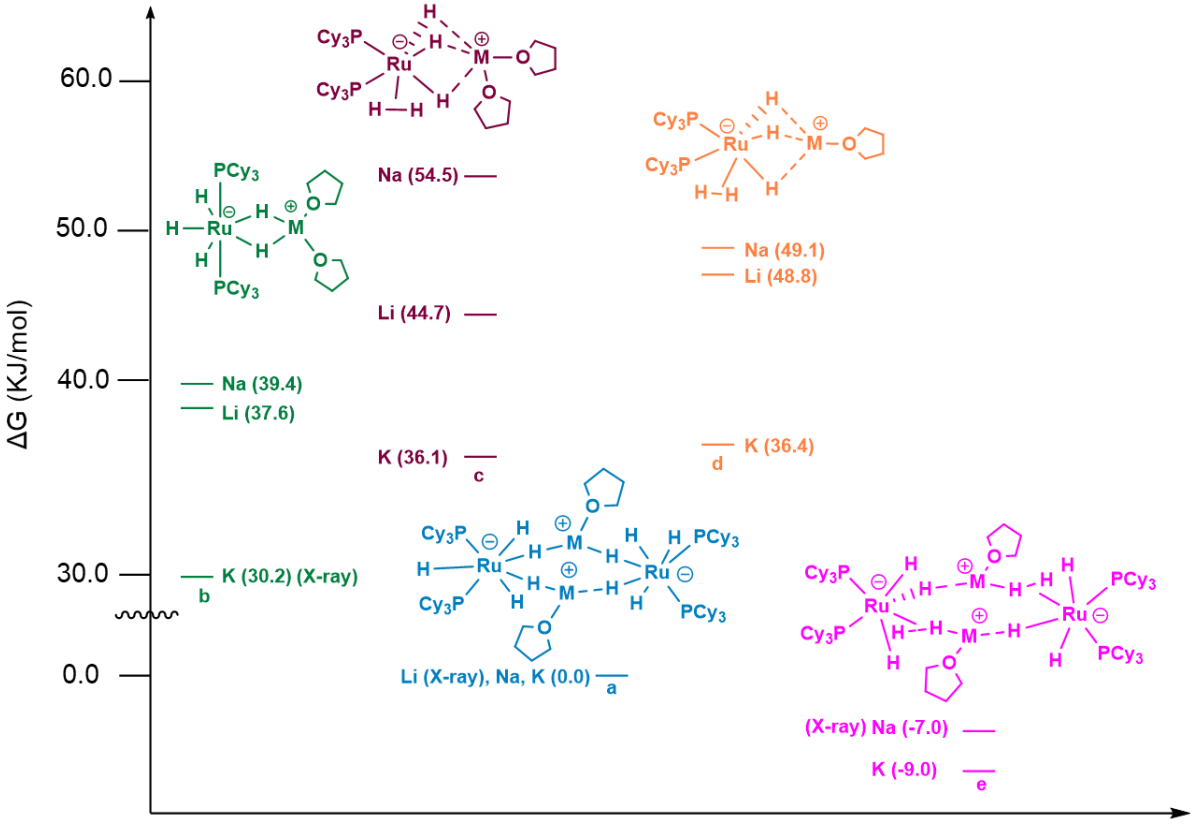

Figure 7. Energy level diagram of different isomers of **2Li-(a-d), 2Na-(a-e) and 2K-(a-e)** optimized by DFT calculations. The optimized complexes corresponding to the X-Ray structure are indicated.

by X-ray diffraction two hydrides are in close contact with a distance of 0.988 Å in excellent agreement with the X-ray distance of 1.00(7) Å between H201 and H203. Such a distance agrees with a dihydrogen ligand bound to ruthenium at the higher limit for an unstretched coordination mode. One of the hydrogens is interacting with sodium at a distance of 2.379 Å again in good agreement with the X-ray value (2.39(5) Å). Finally, the monomer **2K-b** matches perfectly the X-ray data obtained for **2K**, the phosphines being in trans position (177.09°) and the hydrides adopting a pentagonal arrangement.

Beyond the optimized DFT structures **2Li-a**, **2Na-e** and **2K-b** corresponding to the X-ray structures of **2Li**, **2Na** and **2K**, we were able to optimize various other isomers **2Ma-e** represented in Figure 7 for each alkali cation except for **2Li-e** which could not be found as a minimum on the energy surface. Each color represents one structural geometry: blue (a) and pink (e) are dinuclear structures while green (b), brown (c) and yellow (d) are monometallic structures. The Gibbs free energy levels (ΔG, kJ/mol)) were calculated for each species, arbitrary setting 0 for the structures **Li-a**, **Na-a** and **K-a**. While types **a**, **b** and **e** are isomers which have been characterized by X-Ray with the three countercations, this is not the case for the mononuclear species **c** and **d** featuring cis phosphines with a trihydride unit bridging the Ru center and the cation. The difference between **c** and **d** is the number of THF molecules coordinated (2 and 1, respectively) to the alkaline cation.

Finer analysis and energy difference comparison must be taken with care due to the multiple possible conformation of the cyclohexyl substituents of the phosphine moieties and because of the error associated with the entropy, especially when comparing monomeric and dimeric structures. Nonetheless, we observe that in the lithium and sodium cases, the lowest isomers are the dimeric structure with cis-PCy_3 arrangement corresponding to the X-ray analysis. However, the potassium structure **2K-b** is not the lowest minimum found on the potential energy surface. Indeed, **2K-b** is higher in energy by 39.2 kJ.mol^{-1} above **2K-e**, a ruthenium dimer displaying a dihydrogen ligand as obtained for the sodium case. Another dimer **2K-a**, with no dihydrogen ligand was only 9 kJ.mol^{-1} above **2K-e**, whereas two other mononuclear ruthenium species featuring a dihydrogen ligand were located 45.1 and 45.4 kJ.mol^{-1} above **2K-e**.

CONCLUSION

We have synthesized and isolated a series of anionic ruthenium complexes $[RuH_5(PCy_3)_2]^-$ whose structural and spectroscopic properties are highly dependent on the nature of the associated cation: lithium, sodium or potassium. With a significant difference in covalent radii, the cations are able to establish various sets of interactions with the hydrides and the solvent present in the coordination sphere of the metals. Moreover, it is well known that ruthenium is keen to favor dihydrogen bonding, and it is thus not surprising to characterize structures featuring short H-H distances around 1 Å and/or low T_{1min} values. As previously observed,[30] the phosphines are also able to adopt a cis geometry despite their bulkiness. This is remarkably illustrated by the change between the lithium and sodium cases which display a cis configuration versus the potassium structure with trans phosphines as demonstrated by X-ray diffraction. The complexity of the NMR spectra when monitoring the complexes at variable temperatures tends to support the accessibility of various isomers as those calculated by DFT. These highly dynamic structures are very reactive as illustrated by the H/D exchange experiments. In the case of the Morris complexes, deuterium incorporation was only observed for the complexes featuring close proton-hydride contacts between the hydrides and the NH of the crown-ethers.[14] One can conclude on the importance of close ion pair contact to favor such H/D exchange. It will be interesting to investigate the catalytic properties of this series of complexes to evaluate the impact of the various Ru---H---M interactions and the benefits of cation tuning within a polyhydride structure.

EXPERIMENTAL SECTION

General considerations

All manipulations were carried out under an argon atmosphere using either Schlenk techniques or argon filled glove box. Dry and degassed solvents were collected from MBraun solvent purification system (SPS). Deuterated solvents THF-d_8, C_6D_6 and toluene-d_8 were dried over 4 Å molecular sieves, degassed and stored under argon atmosphere. Quick pressure NMR valves and Fischer-Porter vessels were used to carry out reactions under H_2 and D_2. $LiBHEt_3$ (1M in THF), $NaBHEt_3$ (1M in toluene) and KH were purchased from Sigma Aldrich and used as received. $[RuH_2(H_2)_2(PCy_3)_2]$ was synthesized according to literature report.[31] NMR spectra were recorded using Bruker Avance 400 and Avance NEO 600 NMR spectrometers. The ^1H and ^{13}C NMR chemical shifts were referenced to the residual proton and carbon signal of the deuterated solvents, respectively. The ^{31}P and ^7Li NMR spectra were referenced relative to 85% H_3PO_4 aqueous solution and 1M LiCl (external reference) respectively. Chemical shifts are reported in ppm (δ) and coupling constants in Hertz (Hz). The following abbreviations were used, s – singlet, d – doublet, t – triplet, quart – quartet, sept – septet, br-broad and m – multiplet. FTIR-ATR (FTIR – Fourier Transform Infrared Spectroscopy; ATR – Attenuated Total Reflectance) spectra of powder samples **2Li**, **2Na** and **2K** were recorded inside an argon filled glove box using Bruker ALPHA spectrometer in ATR mode on a diamond crystal. Single crystals were diffracted in Bruker Kappa APEX II diffractometer at 100–110 K using Mo Kα radiation (λ = 0.71073 Å) filtered through graphite monochromator. T1 measurements were obtained by conducting inversion recovery experiments at 600 MHz at variable temperatures.[32]

Synthesis and Characterization of $[Li(THF)][RuH_5(PCy_3)_2]$ (2Li)

$[RuH_2(H_2)_2(PCy_3)_2]$ (0.800 g, 1.2 mmol) and 10 equivalents of 1M $LiBHEt_3$ in THF (12 mL, 12.0 mmol) were stirred in THF (5 mL) for 48 h at 298 K under H_2 (1 atm). During the reaction, a colorless precipitate had settled down. After filtration, the colorless precipitate was washed with cold *n*-pentane (2 x 2 mL) and dried under H_2 atm. $[Li(THF)][RuH_5(PCy_3)_2]$ (**2Li**) was isolated as a colorless solid (0.730 g, 81.5 %). Colorless crystals of **2Li**, suitable for X-ray crystallography were obtained by layering a THF solution of **2Li** (5 mL) over *n*-pentane (10 mL) at 298 K over 48 h, under H_2 atm.

^1H NMR (400.13 MHz, 298 K, THF-d_8): δ –9.58 (t, $^2J_{H-P}$ = 14.2 Hz, 5H, Ru-H_5), 1.1–2.1 (m, 66H, Cy_3). ^{31}P NMR (161.98 MHz, 297.9 K, THF-d_8): δ 81.8 (s); $^7Li\{^1H\}$ NMR (155.51 MHz, 298 K, THF-d_8): δ 1.8 (very broad); $^{13}C\{^1$; NMR (100.64 MHz, 298.3 K, THF-d_8): δ 40.9 (t, J_{C-P} = 7.8 Hz, C1), 31.2 (s, C3), 29.4 (t, J_{C-P} = 4.6 Hz, C2), 28.3 (s, C4); T_1(ms, 600 MHz, THF-d_8): 242 (298 K), 209 (273 K), 206 (263 K), 207 (253 K), 217 (243 K), 230 (233 K), 253 (213 K), 347 (193 K).

Synthesis and Characterization of $[Na(THF)][RuH_5(PCy_3)_2]$ (2Na)

$[RuH_2(H_2)_2(PCy_3)_2]$ (0.200 g, 0.299 mmol) and 10 equivalents of 1M $NaBHEt_3$ in toluene (3 mL, 2.99 mmol) were stirred in THF (5 mL) for 24 h at 323 K under H_2 (1 atm). During the reaction, a colorless precipitate had settled down. After filtration, it was washed with cold *n*-pentane (2 x 2 mL) and dried under H_2 atm. $[Na(THF)][RuH_5(PCy_3)_2]$ (**2Na**) was isolated as a colorless solid

(0.180 g, 79 %). Colorless crystals of **2Na**, suitable for X-ray crystallography were obtained by layering a THF solution of **2Na** (5 mL) over *n*-pentane (10 mL) at 298 K over 48 h, under H_2 atm.

^{1}H NMR (600.47 MHz, 298 K, THF-d_8): δ –9.62 (t, $^2J_{H-P}$ = 14.9 Hz, 5H, Ru-H_5), 1.1–2.1 (m, 66H, Cy_3); $^{31}P\{^1H\}$ NMR (243.09 MHz, 298.1 K, THF-d_8): δ 83.0 (s); $^{13}C\{^1H\}$ NMR (151.0 MHz, 273.0 K, THF-d_8): δ 41.0 (t, J_{C-P} = 7.3 Hz, C1), 31.3 (s, C3), 29.5 (t, J_{C-P} = 4.3 Hz, C2), 28.5 (s, C4); T_1(ms, 600 MHz, THF-d_8): 284 (298 K), 232 (273 K), 223 (263 K), 220 (253 K), 229 (243 K), 261 (233 K), 404 (213 K).

Synthesis and Characterization of $[K(THF)_2][RuH_5(PCy_3)_2]$ (2K)

$[RuH_2(H_2)_2(PCy_3)_2]$ (0.400 g, 0.598 mmol) and 10 equivalents of KH (0.240 g, 5.98 mmol) were stirred in THF (10 mL) for 36 h at 323 K under H_2 (1 atm). Upon cooling the reaction mixture, the supernatant solution was filtered using a filter paper cannula. Further addition of THF (2 x 4 mL) to the remaining solid and subsequent filtration led to a saturated solution which produced within 1 hour a white precipitate. After filtration, the precipitate was washed with *n*-pentane (3 x 2 mL) and dried under H_2 atm, giving $[K(THF)_2][RuH_5(PCy_3)_2]$ (**2K**) as a colorless solid (0.300 g, 65 %). Colorless needles of **2K**, suitable for X-ray crystallography were obtained by layering a THF solution of **2K** (5 mL) over *n*-pentane (10 mL) at 298 K over 24 h, under H_2 atmosphere.

^{1}H NMR (400.13 MHz, 298 K, THF-d_8): δ –9.26 (t, $^2J_{H-P}$ = 12.9 Hz, 5H, Ru-H_5), 1.1–2.1 (m, 66H, Cy_3); $^{31}P\{^1H\}$ NMR (243.09 MHz, 298.1 K, THF-d_8): δ 86.3 (s); $^{13}C\{^1H\}$ NMR (151.0 MHz, 294.0 K, THF-d_8): δ 41.1 (t, J_{C-P} = 7.3 Hz, C1), 31.4 (s, C3), 29.6 (t, J_{C-P} = 4.5 Hz, C2), 28.5 (s, 6C, C4); T_1(ms, 600 MHz, THF-d_8): 575 (298 K), 495 (273 K), 476 (253 K), 459 (233 K), 455 (223 K), 457 (213 K), 467 (203 K), 500 (193 K); T_1(ms, 600 MHz, tol-d_8): 204(294.3 K) and 372 (273 K). H-D exchange of RuH_5 with tol-d_8 precluded T_1 measurements below 273 K.

ASSOCIATED CONTENT

Supporting Information

NMR spectral characterization of compounds **2Li**, **2Na** and **2K**, X-ray data collection and structure refinement parameters and summary of DFT calculations and Cartesian coordinates of optimized structures were provided in the supporting information. CCDC numbers for **2Li** (2091981), **2Na** (2091980) and **2K** (2091979). This material is available free of charge via the internet at http://pubs.acs.org.

AUTHOR INFORMATION

Corresponding Author

*Email: sylviane.sabo@lcc-toulouse.fr, sebastien.bontemps@lcc-toulouse.fr

Notes

The authors declare no competing financial interest.

ACKNOWLEGEMENTS

We gratefully acknowledge financial support from CNRS and CEFIPRA on project 5905-1. Yannick Coppel and Christian Bijani are also warmly acknowledged for their contribution in NMR analyses. We were also granted access for this research to the HPC resources of the CALMIP supercomputing center under the allocation 2020-2021-[p0909], Toulouse, France

REFERENCES

1. Esteruelas, M. A.; López, A. M.; Oliván, M., Polyhydrides of Platinum Group Metals: Nonclassical Interactions and σ-Bond Activation Reactions. *Chem. Rev.* **2016,** *116* (15), 8770-8847.
2. Norton, J. R.; Sowa, J., Introduction: Metal Hydrides. *Chem. Rev.* **2016,** *116* (15), 8315-8317.
3. Kubas, G. J., Activation of dihydrogen and coordination of molecular H_2 on transition metals. *J. Organomet. Chem.* **2014,** *751*, 33-49.
4. Galey, B.; Auroux, A.; Sabo-Etienne, S.; Grellier, M.; Dhaher, S.; Postole, G., Impact of the addition of poly-dihydrogen ruthenium precursor complexes on the hydrogen storage properties of the Mg/MgH_2 system. *Sustainable Energy & Fuels* **2018,** *2* (10), 2335-2344.
5. Beguerie, M.; Dinoi, C.; del Rosal, I.; Faradji, C.; Alcaraz, G.; Vendier, L.; Sabo-Etienne, S., Mechanistic Studies on the Catalytic Synthesis of BN Heterocycles (1H-2,1-Benzazaboroles) at Ruthenium. *ACS Catal.* **2018,** *8* (2), 939-948.
6. Bontemps, S.; Vendier, L.; Sabo-Etienne, S., Ruthenium-Catalyzed Reduction of Carbon Dioxide to Formaldehyde. *J. Am. Chem. Soc.* **2014,** *136* (11), 4419-4425.
7. Bontemps, S.; Sabo-Etienne, S., Trapping Formaldehyde in the Homogeneous Catalytic Reduction of Carbon Dioxide. *Angew. Chem. Int. Ed.* **2013,** *52* (39), 10253-10255.
8. Bontemps, S.; Vendier, L.; Sabo-Etienne, S., Borane-Mediated Carbon Dioxide Reduction at Ruthenium: Formation of C_1 and C_2 Compounds. *Angew. Chem. Int. Ed.* **2012,** *51* (7), 1671-1674.
9. Darensbourg, M. Y.; Ash, C. E., Anionic Transition Metal Hydrides. In *Adv. Organomet. Chem.*, O'Malley, B. W., Ed. Academic Press: 1987; Vol. 27, pp 1-50.
10. Plois, M.; Hujo, W.; Grimme, S.; Schwickert, C.; Bill, E.; de Bruin, B.; Pöttgen, R.; Wolf, R., Open-Shell First-Row Transition-Metal Polyhydride Complexes Based on the fac-[RuH3(PR3)3]– Building Block. *Angew. Chem. Int. Ed.* **2013,** *52* (4), 1314-1318.
11. Plois, M.; Wolf, R.; Hujo, W.; Grimme, S., Towards Reagents for Bimetallic Activation Reactions: Polyhydride Complexes with Ru_2H_3, Ru_2ZnH_6, and $Cu_2Ru_2H_6$ Cores. *Eur. J. Inorg. Chem.* **2013,** *2013* (17), 3039-3048.
12. Miloserdov, F. M.; Rajabi, N. A.; Lowe, J. P.; Mahon, M. F.; Macgregor, S. A.; Whittlesey, M. K., Zn-Promoted C–H Reductive Elimination and H_2 Activation via a Dual Unsaturated Heterobimetallic Ru–Zn Intermediate. *J. Am. Chem. Soc.* **2020,** *142* (13), 6340-6349.
13. Gusev, D. G.; Lough, A. J.; Morris, R. H., New Polyhydride Anions and Proton-Hydride Hydrogen Bonding in Their Ion Pairs. X-ray Crystal Structure Determinations of Q[mer-$Os(H)_3(CO)(PiPr_3)_2$], Q = [K(18-crown-6)] and Q = [K(1-aza-18-crown-6)]. *J. Am. Chem. Soc.* **1998,** *120* (50), 13138-13147.
14. Abdur-Rashid, K.; Gusev, D. G.; Lough, A. J.; Morris, R. H., Intermolecular Proton−Hydride Bonding in Ion Pairs: Synthesis and Structural Properties of $[K(Q)][MH_5(PiPr_3)_2]$ (M = Os, Ru; Q = 18-crown-6, 1-aza-18-crown-6, 1,10-diaza-18-crown-6). *Organometallics* **2000,** *19* (5), 834-843.
15. Abdur-Rashid, K.; Gusev, D. G.; Lough, A. J.; Morris, R. H., Synthesis and Characterization of $RuH_2(H_2)_2(PiPr_3)_2$ and Related Chemistry. Evidence for a Bis(dihydrogen) Structure. *Organometallics* **2000,** *19* (9), 1652-1660.
16. Alcaraz, G.; Grellier, M.; Sabo-Etienne, S., Bis sigma-Bond Dihydrogen and Borane Ruthenium Complexes: Bonding Nature, Catalytic Applications, and Reversible Hydrogen Release. *Acc. Chem. Res.* **2009,** *42* (10), 1640-1649.
17. Smith, P. W.; Ellis, S. R.; Handford, R. C.; Tilley, T. D., An Anionic Ruthenium Dihydride $[Cp^*(iPr_2MeP)RuH_2]^-$ and Its Conversion to Heterobimetallic Ru(μ-H)$_2$M (M = Ir or Cu) Complexes. *Organometallics* **2019,** *38* (2), 336-342.
18. Gil-Negrete, J. M.; Hevia, E., Main group bimetallic partnerships for cooperative catalysis. *Chem. Sci.* **2021,** *12* (6), 1982-1992.
19. Davin, L.; Hernán-Gómez, A.; McLaughlin, C.; Kennedy, A. R.; McLellan, R.; Hevia, E., Alkali metal and stoichiometric effects in intermolecular hydroamination catalysed by lithium, sodium and potassium magnesiates. *Dalton Trans.* **2019,** *48* (23), 8122-8130.
20. McWilliams, S. F.; Broere, D. L. J.; Halliday, C. J. V.; Bhutto, S. M.; Mercado, B. Q.; Holland, P. L., Coupling dinitrogen and hydrocarbons through aryl migration. *Nature* **2020,** *584* (7820), 221-226.
21. Broere, D. L. J.; Mercado, B. Q.; Bill, E.; Lancaster, K. M.; Sproules, S.; Holland, P. L., Alkali Cation Effects on Redox-Active

Formazanate Ligands in Iron Chemistry. *Inorg.Chem.* **2018,** *57* (16), 9580-9591.
22. Complex **2Li** was first generated by using a lithium phosphino-borate compound [Li(OEt$_2$)][o-iPr$_2$P-C$_6$H$_4$-C$_8$H$_{14}$-B-H] acting as a lithium hydride transfer agent that we recently reported. The NMR data match those obtained when reacting the bis(dihydrogen) complex **1** with a 1M LiBHEt3 solution in THF, see: Ayyappan, R.; Coppel, Y.; Vendier, L.; Ghosh, S.; Sabo-Etienne, S.; Bontemps, S., Synthesis and reactivity of phosphine borohydride compounds. *Chem. Commun.* **2021**, *57*, 375-378.
23. Cordero, B.; Gómez, V.; Platero-Prats, A. E.; Revés, M.; Echeverría, J.; Cremades, E.; Barragán, F.; Alvarez, S., Covalent radii revisited. *Dalton Trans.* **2008,** (21), 2832-2838.
24. Sellmann, D.; Gottschalk-Gaudig, T.; Heinemann, F. W., Transition Metal Complexes with Sulfur Ligands. 130.1 Synthesis, Structure, and Reactivity of the Sulfur-Rich Ruthenium Hydride Complexes [Ru(H)(PR$_3$)('S4')]- and the η^2-H$_2$ Complex [Ru(H$_2$)(PCy$_3$)('S4')] (R = Ph, iPr, Cy; 'S4'2- = 1,2-Bis((2-mercaptophenyl)thio)ethane(2$^-$)). *Inorg.Chem.* **1998,** *37* (16), 3982-3988.
25. Sellmann, D.; Prakash, R.; Heinemann, F. W.; Moll, M.; Klimowicz, M., Heterolytic Cleavage of H$_2$ at a Sulfur-Bridged Dinuclear Ruthenium Center. *Angew. Chem., Int. Ed.* **2004,** *43* (14), 1877-1880.
26. Chan, A. S. C.; Shieh, H.-S., New synthesis and molecular structure of potassium trihydridotris(triphenylphosphine)ruthenate. *J. Chem. Soc., Chem. Commun.,* **1985,** (20), 1379-1380.
27. Drouin, S. D.; Amoroso, D.; Yap, G. P. A.; Fogg, D. E., Multifunctional Ruthenium Catalysts: A Novel Borohydride-Stabilized Polyhydride Complex Containing the Basic, Chelating Diphosphine 1,4-Bis(dicyclohexylphosphino)butane and Its Application to Hydrogenation and Murai Catalysis. *Organometallics* **2002,** *21* (6), 1042-1049.
28. Gilbert-Wilson, R.; Field, L. D.; Bhadbhade, M., Ruthenium Hydrides Containing the Superhindered Polydentate Polyphosphine Ligand P(CH$_2$CH$_2$P*t*Bu$_2$)$_3$. *Inorg.Chem.* **2014,** *53* (23), 12469-12479.
29. Crabtree, R. H., Dihydrogen Complexation. *Chem. Rev.* **2016,** *116* (15), 8750-8769.
30. Gloaguen, Y.; Alcaraz, G.; Pécharman, A.-F.; Clot, E.; Vendier, L.; Sabo-Etienne, S., Phosphinoborane and Sulfidoborohydride as Chelating Ligands in Polyhydride Ruthenium Complexes: Agostic σ-Borane versus Dihydroborate Coordination. *Angew. Chem., Int. Ed.* **2009,** *48* (16), 2964-2968.
31. Borowski, A. F.; Sabo-Etienne, S.; Christ, M. L.; Donnadieu, B.; Chaudret, B., Versatile Reactivity of the Bis(dihydrogen) Complex [RuH$_2$(H$_2$)$_2$(PCy$_3$)$_2$] toward Functionalized Olefins: Olefin Coordination versus Hydrogen Transfer via the Stepwise Dehydrogenation of the Phosphine Ligand. *Organometallics* **1996,** *15* (5), 1427-1434.
32. Hamilton, D. G.; Crabtree, R. H., An NMR method for distinguishing classical from nonclassical structures in transition metal polyhydrides. *J. Am. Chem. Soc.* **1988,** *110* (13), 4126-4133.